 DOI: 10.19600/j.cnki.issn2152 - 3924.2026.03.002

Evaluation of Nardosinone Accumulation in *Nardostachys jatamansi* Based on Expression of Key Leaf Genes

Jianli JIMU, Zina LI, Shaoshan ZHANG, Huachun SHENG, Yuan LIU, Wenbing LI*

School of Pharmacy and Food Science, Southwest Minzu University, Chengdu 610041, China; Sichuan Provincial Engineering Laboratory for Conservation and Utilization of Qiang-Yi Medicinal Resources, Chengdu 610225, China; Key Laboratory of National Ethnic Affairs Commission for Preservation and Utilization of Ethnomedicinal Resources in Qinghai-Tibet Plateau, Chengdu 610225, China

Abstract [**Objectives**] To analyze the gene expression networks across distinct tissues of *Nardostachys jatamansi* and elucidate the correlation between key gene expression levels in leaves and nardosinone accumulation in medicinal rhizomes, providing a technical foundation for rapid monitoring of bioactive compound accumulation. [**Methods**] Transcriptome sequencing coupled with Weighted Gene Co-expression Network Analysis (WGCNA) was employed to construct gene co-expression networks, Ultra-performance Liquid Chromatography (UPLC) was utilized to quantify nardosinone content across various growth stages. Real-Time Quantitative Polymerase Chain Reaction (RT-qPCR) was integrated to validate spatiotemporal relationships between key gene expression profiles and nardosinone accumulation patterns. [**Results**] Among seven co-expression modules, the blue module demonstrated an exceptionally strong correlation with nardosinone content ($r = 0.993$, $p = 1.2 \times 10^{-15}$). This module encompassed pivotal genes such as *NjDXS3* and *NjTPS22*. Three-year-old *N. jatamansi* plants reached peak nardosinone accumulation in September, with leaf expression levels of *NjDXS3* closely mirroring this accumulation trend, whereas *NjTPS22* expression exhibited minimal temporal variation. A critical threshold ratio exceeding 4.5 for *NjDXS3*/*NjTPS22* expression in leaves signaled peak nardosinone concentrations. [**Conclusions**] By monitoring the expression ratio of *NjDXS3* to *NjTPS22* in leaves, the accumulation status of bioactive compounds in medicinal organs can be non-invasively assessed, offering a novel methodology for quality evaluation of *N. jatamansi* crude drugs.

Key words *Nardostachys jatamansi*, Gene expression level, Bioactive compound accumulation, Nardosinone, Evaluation method

1 Introduction

Nardostachys jatamansi (Valerianaceae), known as "Gansong", comprises dried roots and rhizomes, and serves as a traditional medicinal plant utilized by Tibetan, Han, Mongolian, and other ethnic groups in China. Characterized by a pungent-sweet flavor and warm nature, it exhibits efficacy in regulating qi, alleviating pain, and invigorating spleen function, Topically, it dispels dampness and reduces swelling, while clinically applied for epigastric distension, anorexia, and vomiting, and externally manages toothache and beriberi-related edema[1]. Simultaneously, it constitutes a core ingredient in products such as Tibetan ritual incense and Buchang Wenxin Granules (an anti-arrhythmia formulation), with wild resources predominantly distributed in the eastern Tibetan regions of Sichuan, Tibet, and Qinghai within the Qinghai-Tibet Plateau[2].

With escalating varieties and sales of Chinese patent medicines—including Songbuli Oral Liquid and Shangtongning Capsules—alongside Tibetan incense and daily chemical products, the demand for *N. jatamansi* exhibits a year-on-year upward trajectory. Current wild resources are progressively depleting, and imported supplies are diminishing, collectively failing to meet market demands. Concurrently, owing to stringent ecological requirements (altitude 2 800 - 4 800 m) and immature cultivation techniques, resource acquisition solely relies on wild harvesting. Amplified demand and unregulated harvesting have pushed wild populations toward endangerment[3-4], subsequently listing them under *CITES* (*Convention on International Trade in Endangered Species*), the *IUCN Red List of Threatened Species*, *and China's List of National Key Protected Wild Plants*[5-7].

Consequently, protecting *N. jatamansi* wild resources is critically urgent. Over a decade, our research group has concentrated on conservation and utilization, achieving substantial progress in wild-simulated ecological cultivation, breeding, and novel material selection via the Qinghai-Tibet Plateau research base. The absence of a multidimensional quality evaluation system tailored to traditional Chinese medicine hampers systematic assessment of "wild-simulated" quality, impeding the promotion of cultivation technologies.

Building on prior work, this study establishes a multidimensional quality evaluation framework—integrating morphological traits, chemical composition, and gene expression—as a benchmark to assess wild-simulated *N. jatamansi* quality; concurrently identifying key genes governing quality traits, developing an evaluation model linking bioactive compound content to gene expression networks, and furnishing scientific groundwork to advance cultivation and rapid quality appraisal, thereby enabling artificial cultivation to supplant wild harvesting.

2 Materials and methods

2.1 Materials Wild-simulated and wild *N. jatamansi* specimens were collected between May and September 2025: Wild-simulated plants originated from the Qinghai-Tibet research base at

Received: March 13, 2026 Accepted: May 30, 2026

Supported by Sichuan Provincial Key R&D Program (2024YFFK0190); Fundamental Research Funds for the Central Universities, Southwest Minzu University (ZYN2026258).

Jianli JIMU, master's degree candidate. * Corresponding author. Wenbing LI, doctoral degree, associate researcher.

Southwest Minzu University in Qiongxi Town, Hongyuan County, with seeds sourced from wild plants at Lower Halamashan Mountain in Anqu Town; whole plants were transplanted at seedling stage for wild-simulated cultivation. Specimens comprised three-year-old cultivated materials, authenticated by Professor Liu Yuan from Southwest Minzu University as *N. jatamansi* (Valerianaceae).

2.2 Instruments and reagents Waters H-class UPLC (Waters Corporation, USA), ATX124 analytical balance (d = 0.000 1 g, Shimadzu, Japan); Nardosinone reference standard (Batch No. 111832-202205, purity 99.6%) procured from Lemetian Pharmaceutical Biotechnology Co., Ltd.; RNA extraction kit (FastPure® Universal Plant Total RNA Isolation Kit), reverse transcription kit [HiScript® II QRT SuperMix for qPCR (+gDNA wiper)], and RT-qPCR kit [2×Taq Master Mix (Dye Plus)] all obtained from Nanjing Vazyme Biotech Co., Ltd.

2.3 Construction of sesquiterpenoid expression network in *N. jatamansi* Utilizing full-length transcriptome sequencing data from Illumina and PacBio platforms, weighted gene co-expression network analysis (WGCNA) was applied to identify sesquiterpenoid biosynthesis-associated modules and target genes. Data analysis was executed using R with the WGCNA package, and visualization implemented in Python.

2.4 Real-Time Quantitative Polymerase Chain Reaction (RT-qPCR) Leaf tissues from diverse growth stages were sampled; total RNA was extracted following the FastPure® Universal Plant Total RNA Isolation Kit (RC441) protocol, and cDNA synthesized using the accompanying reverse transcription kit. Universal primers for *NjDXS3* and *NjTPS22* were designed via Primer3Plus online. RT-qPCR cycling protocol: initial denaturation at 95 ℃ for 3 min; followed by 32 cycles of denaturation (95 ℃, 15 sec), annealing (55 ℃, 15 sec), and extension (72 ℃, 30 sec); with a final extension at 72 ℃ for 5 min. *NjActin* served as the reference gene, and experiments included three technical replicates. Reaction mixture comprised: 25 μL 2×Taq Master Mix (Dye Plus), 2 μL each of forward and reverse primers (10 μmol/L), 1 μL cDNA template, and 20 μL RNase-free dH_2O.

2.5 Quantification of active components including nardosinone

2.5.1 Preparation of reference solutions. Accurately weighed reference standards of nardosinone, isonardosinone, and nardin C were dissolved in methanol to prepare solutions of varying concentrations.

2.5.2 Preparation of sample solutions. Approximately 0.5 g of powdered *N. jatamansi* was placed in a sealed conical flask; precisely 20 mL methanol was added, and the weight recorded. Ultrasonic extraction (500 W, 40 kHz) was performed for 45 min; after cooling, methanol replenished weight loss, solutions shaken uniformly, filtered, and the filtrate passed through 0.22 μm microporous membrane.

2.5.3 Chromatographic conditions. Column: ACQUITY UPLC® HSS T3 (2.1 mm×100 mm, 1.8 μm); mobile phase: acetonitrile (A) and 0.1% phosphoric acid aqueous solution (B); with gradient elution: 0–8 min, 30%–55% A; 8–15 min, 55%–60% A; 15–25 min, 60% A; 25–28 min, 60%–90% A; injection volume: 2.0 μL; flow rate: 0.2 mL/min; column temperature: 30 ℃; detection wavelength: 254 nm.

2.5.4 Methodological validation. Based on the chromatography setup and solutions, method validation assessed linearity, repeatability, precision, stability, recovery, limit of detection, and limit of quantitation; with results summarized in Table 1, indicating robust method performance.

Table 1 Methodological validation for three sesquiterpenoid chemicals

Chemical component	LOD μg/mL	LOQ μg/mL	Standard curve	Correlation coefficient (R^2)	Linear range μg/mL	Recovery rate/accuracy (%, n=3)	Precision (*RSD*%, n=6)	Stability (*RSD*%)	System suitability (*RSD*%, n=6)
Nardosinone	0.59	1.97	y=17 955 059.65x+137 374.20	0.999 9	13.4–1 450.0	98.10	0.41	1.13	1.10
Nardin C	1.29	4.30	y=8 250 215.37x−19 682.80	0.999 7	11.7–93.8	101.08	1.41	1.45	1.43
Isonardosinone	0.65	2.15	y=13 003 028.02x+11 509.69	0.999 6	12.1–72.3	99.32	1.59	1.47	0.92

2.5.5 Sample content determination. Precisely 2 μL reference and sample solutions were injected into the liquid chromatograph for quantification.

3 Results and analysis

3.1 Weighted Gene Co-expression Network Analysis (WGCNA) Employing WGCNA, this study utilized an initial dataset of 26 482 high-quality full-length transcripts derived from PacBio SMRT sequencing, encompassing expression profiles across the full growth cycle in roots, rhizomes, leaves, and flowers. To enhance network robustness and biological relevance, stringent quality control filtered raw expression matrices: Transcripts with low expression (FPKM < 1 in all samples) and minimal cross-sample variance (standard deviation ≤ 1) were excluded, eliminating technical noise and background expression; concurrently, poorly annotated sequences failing to map to the *N. jatamansi* reference genome were discarded. Post-filtering, 7 708 high-confidence genes with stable dynamic expression patterns and functional annotation potential were retained for unsupervised clustering analysis. A scale-free topological network was established via soft-thresholding (power = 12, R^2 = 0.92), partitioning genes into seven distinct co-expression modules—designated blue, brown, yellow, green, red, cyan, and black—using hierarchical clustering and dynamic tree-cutting algorithms, with module sizes ranging from 282 to 2 520 genes (Fig. 1).

3.2 Module-trait correlation analysis based on measured bioactive compound content To probe key regulatory units linked to target metabolite accumulation, module-trait correlation

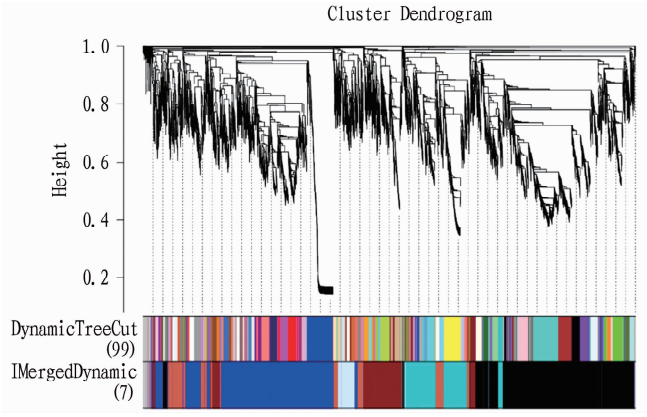

NOTE Identical colors indicate identical modules; correlated modules are merged.

Fig. 1 Gene module clustering dendrogram based on topological overlap

analysis was performed using phenotypic variables derived from LC-MS/MS quantification of three core sesquiterpenoids: nardosinone, nardin C, and isonardosinone (Fig. 2A). Results revealed that among all seven modules, only the blue module exhibited robust positive correlations with all three compounds ($|r| \geqslant 0.99$, $p \approx 0$), notably achieving $r = 0.993$ ($p = 1.2 \times 10^{-15}$) for nardosinone, indicating that its gene co-expression patterns closely align with the biosynthesis dynamics of terpenoid end-products (Fig. 2B).

3.3 Screening of key genes In-depth dissection of the blue module identified 1 256 genes, including 29 annotated as terpene synthase (TPS) family members, spanning TPS-a, TPS-b, and TPS-g subfamilies, predominantly featuring dual domains (RRX8W, DDXXD) and metal-binding motifs; additionally, 77 cytochrome P450 monooxygenase (CYP) genes—subcategorized as NjCYP71D, NjCYP76AH, *etc.*—were enriched, with 43 showing significant co-expression with upstream MVA/MEP pathway

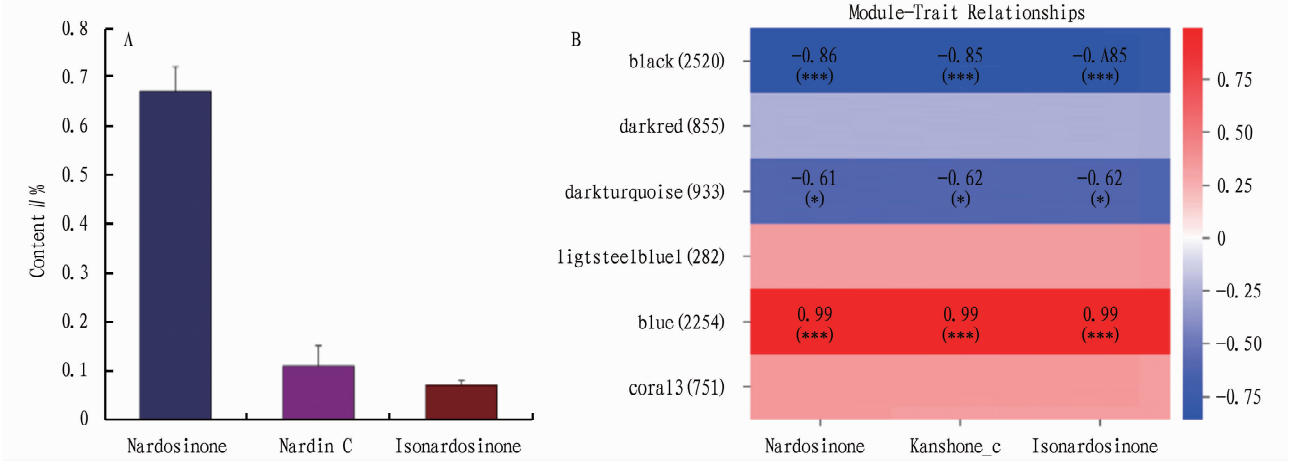

NOTE A. Content of nardosinone, nardin C, and isonardosinone in June wild-simulated *Nardostachys jatamansi*; B. Module-trait relationship.

Fig. 2 Module-trait correlation analysis based on measured bioactive compound content

enzymes (*e. g.*, NjHMGR, NjDXS, NjIDI; Pearson $r > 0.82$, FDR-adjusted $p < 0.01$) (Fig. 3). These genes exhibited predominant expression in roots and lower levels in leaves. Notably, *NjTPS22* had high expression in roots but the lowest expression among all known TPS members in leaves. *NjDXS3* analogously displayed root-specific expression patterns yet maintained substantial expression in leaves. Thus, *NjDXS3* and *NjTPS22* were selected as key genes for evaluating accumulation in subterranean organs via leaf expression measurement.

3.4 Correlation between leaf expression levels of *NjDXS*3 and *NjTPS*22 and root nardosinone content across growth periods To systematically elucidate spatiotemporal dynamics and molecular regulation of sesquiterpenoid accumulation, multitemporal sampling analyzed medicinal organs (roots and rhizomes) and vegetative organs (leaves) across growth stages (May-September), focusing on nardosinone content dynamics while concurrently detecting transcription levels of two functional genes—*NjDXS3* (encoding MEP pathway rate-limiting enzyme 1-deoxy-D-xylulose-5-phosphate synthase 3) and *NjTPS22* (encoding a sesquiterpene synthase)—in leaves. Findings indicated that three-year-old

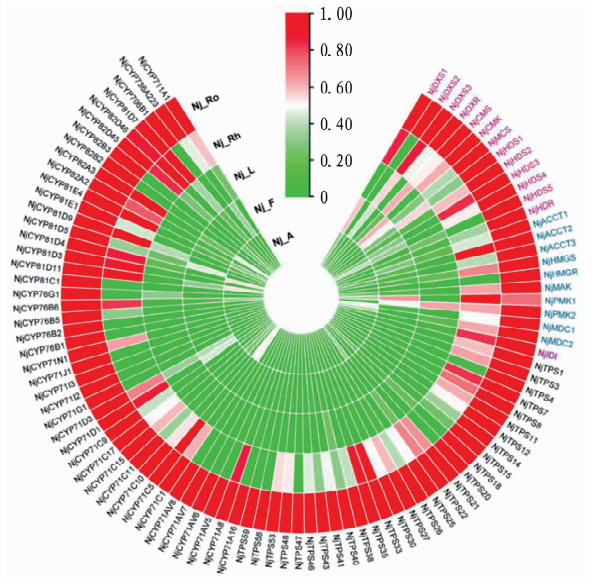

Fig. 3 Sesquiterpenoid biosynthesis pathway and key gene distribution in *Nardostachys jatamansi*

plants peaked in nardosinone accumulation in September; concurrently, leaf transcription of *NjDXS3* significantly upregulated, mirroring root nardosinone seasonal dynamics; in contrast, *NjTPS22* expression remained relatively stable through the observation period, with no statistically significant fluctuation in September (Fig. 4). These results demonstrate the feasibility of estimating subterranean bioactive content via leaf transcript levels, with a ratio threshold of 4.5 for *NjDXS3/NjTPS22* signaling peak nardosinone concentrations (Fig. 4).

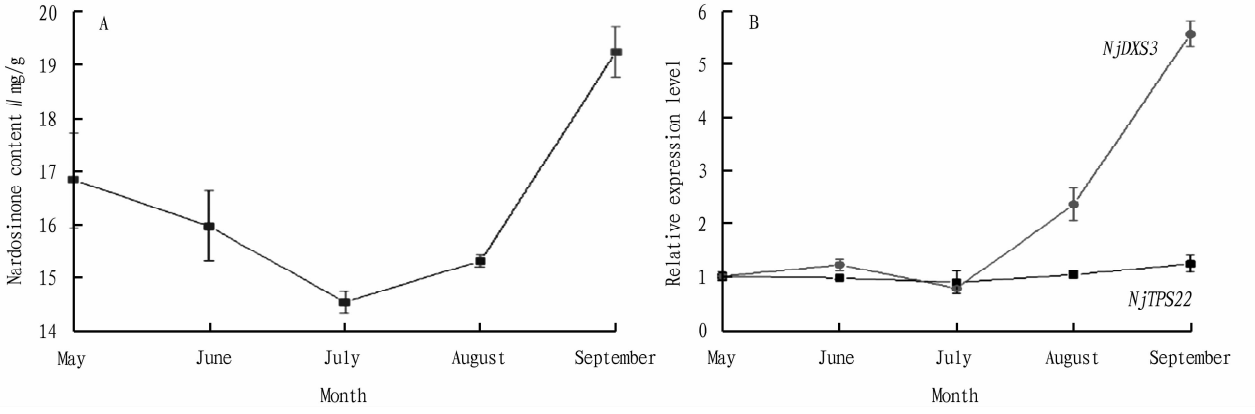

NOTE A. Nardosinone content variation from May to September; B. Dynamic expression of key genes.

Fig. 4 Spatially and temporally specific nardosinone accumulation and key gene expression

4 Discussion

Plant sesquiterpenoids are primarily biosynthesized via the MEP and MVA pathways, which synthesize precursor molecules IPP and DMAPP. These pathways engage in inter-organellar substrate exchange and collectively regulate terpenoid secondary metabolism[8-9]. The MEP pathway operates within plastids, initiating with pyruvate and glyceraldehyde-3-phosphate as substrates. It proceeds through seven enzymatic steps catalyzed by DXS (1-deoxy-D-xylulose-5-phosphate synthase), DXR (1-deoxy-D-xylulose-5-phosphate reductoisomerase), CMS (2-C-methyl-D-erythritol 2,4-cyclodiphosphate synthase), CMK (4-diphosphocytidyl-2-C-methyl-D-erythritol kinase), MCS (2-C-methyl-D-erythritol 2,4-cyclodiphosphate synthase), HDS (1-hydroxy-2-methyl-2-(E)-butenyl-4-diphosphate synthase), and HDR (1-hydroxy-2-methyl-2-(E)-butenyl-4-diphosphate reductase), ultimately yielding isopentenyl diphosphate (IPP) and its isomer dimethylallyl diphosphate (DMAPP). Conversely, the cytosolic MVA pathway commences with acetyl-CoA and involves sequential catalysis by AACT (acetoacetyl-CoA thiolase), HMGS (hydroxymethylglutaryl-CoA synthase), HMGR (hydroxymethylglutaryl-CoA reductase—the key rate-limiting step), MVK (mevalonate kinase), PMK (phosphomevalonate kinase), MDC (mevalonate diphosphate decarboxylase), and IDI (isopentenyl diphosphate isomerase), likewise producing IPP and DMAPP[10-12]. Interpathway crosstalk enables precursor exchange across organelles; specifically, IPP synthesized in plastids can be transported to the cytosol to participate in sesquiterpene backbone assembly, thereby achieving coordinated regulation of metabolic flux.

DXS3 (1-deoxy-D-xylulose-5-phosphate synthase 3) encodes the first rate-limiting enzyme in the MEP pathway. It catalyzes the condensation of pyruvate and glyceraldehyde-3-phosphate to form 1-deoxy-D-xylulose-5-phosphate (DXP). This initial reaction constitutes the gateway to chloroplast-derived isoprenoid unit (IPP/DMAPP) biosynthesis in plant terpenoid metabolism[13-15]. In terpenoid-accumulating medicinal plants such as *N. jatamansi*, the MEP pathway primarily supplies monoterpene and sesquiterpene precursors. Its activity in non-photosynthetic tissues like roots and rhizomes is dynamically fine-tuned through transcriptional regulation. Studies demonstrate that the DXS gene family exhibits multiple paralogous members in higher plants (*e.g.*, 7 in Arabidopsis, 5 in rice), with distinct members displaying tissue-specific expression patterns and functional divergence: DXS1 predominantly expresses in green tissues and governs photosynthetic pigment biosynthesis; DXS2 responds to mechanical injury or hormonal signals to participate in defensive terpenoid induction; whereas DXS3 shows preferential expression in roots, tubers, or secretory structures and positively correlates with secondary metabolite accumulation (*e.g.*, sesquiterpenes, diterpene resin acids)[16-18]. In this study, DXS3 emerged as a core hub gene within the blue co-expression module. Its expression abundance demonstrated high synchrony with nardosinone, nardin C, and isonardosinone accumulation, suggesting its specialized role in modulating MEP pathway flux allocation in *N. jatamansi* roots, thereby influencing downstream sesquiterpene backbone supply capacity.

IPP and DMAPP undergo condensation reactions catalyzed by prenyltransferases (PTs). Notably, farnesyl diphosphate synthase (FPPS) specifically catalyzes the sequential condensation of one DMAPP molecule with two IPP molecules to yield C15 farnesyl diphosphate (FPP)—the universal direct precursor for all sesquiterpenoid skeletons[19-21]. TPS22 (terpene synthase 22) belongs to the TPS-b subfamily of plant terpene synthases. Its encoding gene is designated *NjTPS22* in *N. jatamansi*. Utilizing FPP as its im-

mediate substrate and requiring Mg^{2+} or Mn^{2+} as cofactors, this enzyme orchestrates complex catalytic reactions—including ionization, cyclization, and rearrangement—to generate diverse sesquiterpene carbon skeletons[22-24]. In summary, DXS3 functions upstream in sesquiterpenoid biosynthesis, whereas TPS22 operates downstream. Both are predominantly expressed in roots and synergistically regulate bioactive compound accumulation. This investigation elucidated their spatiotemporal expression patterns in relation to nardosinone accumulation, demonstrating that monitoring *NjDXS3* and *NjTPS22* expression levels in leaves enables non-invasive assessment of bioactive compound accumulation in subterranean medicinal organs.

References

[1] LEI YY, MA Z, WEI J, *et al*. Identification of GSK3 family and regulatory effects of brassinolide on growth and development of *Nardostachys jatamansi*[J]. China Journal of Chinese Materia Medica, 2025, 50(2): 395-403. (in Chinese).

[2] LI Y, JIN Q, QUN P, *et al*. Botanical name textual research of traditional medicinal plant *Nardostachys jatamansi*[J]. Journal of Chinese Medicinal Materials, 2017, 40(6): 1474-1477. (in Chinese).

[3] DHIMAN N, KUMAR A, KUMAR D, *et al*. De novo transcriptome analysis of the critically endangered alpine Himalayan herb *Nardostachys jatamansi* reveals the biosynthesis pathway genes of tissue-specific secondary metabolites[J]. Scientific Reports, 2020, 10(1): 17186.

[4] KAUR H, LEKHAK MM, CHAHAL S, *et al*. *Nardostachys jatamansi* (D. Don) DC.: An invaluable and constantly dwindling resource of the Himalayas[J]. South African Journal of Botany, 2020, 135: 252-267.

[5] ANONYMOUS. IUCN analyses of proposals to amend the CITES appendices prepared by IUCN Species Commission and the TRAFFIC Network [C]//Proceedings of the Tenth Meeting of the Conference of the Parties to CITES. Gland: IUCN, 1997.

[6] VED D, SAHA D, RAVIKUMAR K, *et al*. *Nardostachys jatamansi*[R]. The IUCN Red List of Threatened Species, 2015: e. T50126627A50131395.

[7] DHIMAN N, BHATTACHARYA A. *Nardostachys jatamansi* (D. Don) DC.: Challenges and opportunities of harnessing the untapped medicinal plant from the Himalayas[J]. Journal of Ethnopharmacology, 2020, 246: 112211.

[8] FENG M, CHEN C, QU-BIE J, *et al*. Metabolome and transcriptome associated analysis of sesquiterpenoid metabolism in *Nardostachys jatamansi* [J]. Frontiers in Plant Science, 2022, 13: 1041321.

[9] KUZUYAMA T. Biosynthetic studies on terpenoids produced by Streptomyces[J]. The Journal of Antibiotics, 2017, 70(7): 811-818.

[10] ALICANDRI E, PAOLACCI AR, OSADOLOR S, *et al*. On the evolution and functional diversity of terpene synthases in the *Pinus* species: A review[J]. Journal of Molecular Evolution, 2020, 88(3): 253-283.

[11] LI M, GOU Y, SHENG H, *et al*. Multi-omics analysis elucidates sesquiterpenoid compounds and identifies IrTPS3 as a key multifunctional terpene synthase in roots and rhizomes of *Inula racemosa*[J]. Annals of Botany, 2026: mcag070.

[12] VRANOVÁ E, COMAN D, GRUISSEM W. Network analysis of the MVA and MEP pathways for isoprenoid synthesis[J]. Annual Review of Plant Biology, 2013, 64: 665-700.

[13] LICHTENTHALER HK. The 1-deoxy-D-xylulose-5-phosphate pathway of isoprenoid biosynthesis in plants[J]. Annual Review of Plant Biology, 1999, 50(1): 47-65.

[14] TIAN S, WANG D, YANG L, *et al*. A systematic review of 1-deoxy-D-xylulose-5-phosphate synthase in terpenoid biosynthesis in plants[J]. Plant Growth Regulation, 2022, 96(2): 221-235.

[15] GAWRILJUK VO, OERLEMANS R, REDDEM ER, *et al*. 1-Deoxy-D-xylulose 5-phosphate synthase: Structural perspectives on an essential enzyme in isoprenoid biosynthesis[J]. Journal of Structural Biology, 2025: 108236.

[16] KIM BR, KIM SU, CHANG YJ. Differential expression of three 1-deoxy-D-xylulose-5-phosphate synthase genes in rice[J]. Biotechnology Letters, 2005, 27(14): 997-1001.

[17] YOU MK, LEE YJ, KIM JK, *et al*. The organ-specific differential roles of rice DXS and DXR, the first two enzymes of the MEP pathway, in carotenoid metabolism in Oryza sativa leaves and seeds[J]. BMC Plant Biology, 2020, 20(1): 167.

[18] DE LUNA-VALDEZ L, CHENGE-ESPINOSA M, HERNÁNDEZ-MUOZ A, *et al*. Reassessing the evolution of the 1-deoxy-D-xylulose 5-phosphate synthase family suggests a possible novel function for the DXS class 3 proteins[J]. Plant Science, 2021, 310: 110960.

[19] ZHANG YB, JIAO D, SHEN CJ, *et al*. Plant prenyltransferases: Diversity, catalytic activities, mechanisms, and application in heterologous production of prenylated natural products[J]. Journal of Integrative Plant Biology, 2026, 68(4): 869-902.

[20] MITSUHASHI T, ABE I. Chimeric terpene synthases possessing both terpene cyclization and prenyltransfer activities[J]. ChemBioChem, 2018, 19(11): 1106-1114.

[21] WALLRAPP FH, PAN JJ, RAMAMOORTHY G, *et al*. Prediction of function for the polyprenyl transferase subgroup in the isoprenoid synthase superfamily[J]. Proceedings of the National Academy of Sciences of the United States of America, 2013, 110(13): E1196-E1204.

[22] MILLER DJ, ALLEMANN RK. Sesquiterpene synthases: Passive catalysts or active players[J]. Natural Product Reports, 2012, 29(1): 60-71.

[23] DEGENHARDT J, KÖLLNER TG, GERSHENZON J. Monoterpene and sesquiterpene synthases and the origin of terpene skeletal diversity in plants[J]. Phytochemistry, 2009, 70(15-16): 1621-1637.

[24] DURAIRAJ J, DI GIROLAMO A, BOUWMEESTER HJ, *et al*. An analysis of characterized plant sesquiterpene synthases[J]. Phytochemistry, 2019, 158: 157-165.

(From page 5)

[8] AL-MOHAIMEED AM, EL-TOHAMY MF, ALI MGH, *et al*. Investigating the stability of a cerebral vasodilator drug using chromatographic methods: Evaluation of methods' practicality and environmental aspects [J]. Journal of Chromatography B, 2024, 1249: 124371.

[9] NEKKALAPUDI AR, NAVULURI S, PIPPALLA S. Eco-friendly stability-indicating HPLC method for related compounds in pemetrexed ditromethamine (antineoplastic agent) for injection[J]. Journal of AOAC International, 2024, 107(3): 415-429.

[10] National Pharmacopoeia Commission. Pharmacopoeia of the People's Republic of China 2025 edition: Part II[S]. Beijing: China Medical Science Press, 2025: 428. (in Chinese).